Solar PV-Based Scalable DC Microgrid for Rural Electrification in Developing Regions

Mashood Nasir, Hassan Abbas Khan, *Member, IEEE*, Arif Hussain, Laeeq Mateen, and Nauman Ahmad Zaffar, *Member, IEEE*

***Abstract*—In this paper, we detail the design, analysis, and implementation of a highly distributed off-grid solar photovoltaic dc microgrid architecture suitable for rural electrification in developing countries. The proposed architecture is superior in comparison with existing architectures for rural electrification because of its 1) generation and storage scalability, 2) higher distribution efficiency (because of distributed generation and distributed storage for lower line losses), 3) ability to provide power for larger communal loads without the requirement for large, dedicated generation by extracting the benefit of usage diversity, and 4) localized control by using the hysteresis-based voltage droop method, thus eliminating the need for a central controller. The proposed microgrid architecture consists of several nanogrids capable of the self-sustained generation, storage, and bidirectional flow of power within the microgrid. Bidirectional power flow and distributed voltage droop control are implemented through the duty cycle control of a modified flyback converter. A detailed analysis in terms of power flow, loss, and system efficiency was conducted by using the Newton–Raphson method modified for dc power flow at varying distribution voltages, conductor sizes, and schemes of interconnection among the contributing nanogrids. A scaled-down version of the proposed architecture with various power sharing scenarios was also implemented on hardware, and yielded satisfactory results.**

***Index Terms*—DC microgrids, distributed generation, Newton–Raphson method, rural electrification, solar PV.**

I. Introduction

CURRENTLY used power systems are primarily based on the constraints on distribution systems that were imposed over a century ago. AC power systems enable efficient transformation of voltage from one level to another, allowing power to be carried for long distances with minimum line losses [1]. This has rendered AC power networks the preferred choice for power transmission and distribution. However, limited funds for the construction of large power plants and the high cost of long-distance transmission lines are among the hurdles to meeting growing energy demands, especially in regions that have not been electrified.

According to the International Energy Agency (IEA), 1.3 billion people living in developing countries, i.e., ∼17.5% of the world's population, do not have access to electricity [2]. The development of mega projects for the rural electrification of these communities in developing countries is constrained by the limitation of resources. Alternatively, various standalone solar photovoltaic (PV) systems have been incorporated as a stop-gap measure to provide rural residents with basic electricity [3], [4]. These systems generally provide between a few watts to a few tens of watts for an average rural house. However, these standalone solutions are suboptimal, as without resource sharing, they do not take advantage of electricity usage diversity. These regions need ample electricity to bear communal loads for facilities such as schools, basic health units and water filtration plants.

Fortunately, most regions in Southeast Asia and Africa receive abundant sunlight (above 5.5 kWhr/m^2/day for most regions) [5], [6]. This makes solar photovoltaic (PV) generation an attractive alternative to conventional electricity generation. Compared with traditional AC distribution, DC microgrids are significantly more efficient due to the absence of DC-to-AC or AC-to-DC conversion when implemented using DC-distributed generation (DG). These systems have an end-to-end efficiency of approximately 80% (for DC loads), compared with an efficiency of 60% with AC microgrids [7]–[9]. Therefore, the focus of this study is low voltage direct current (LVDC) distribution, where costly up-conversions (to kV range) and subsequent down-conversions are not required due to shorter distribution distances at the village level. These factors, along with the decreasing cost of solar PV panels, advancements in battery technology, and the influx of robust power electronic devices, makes solar PV technology highly suitable for distributed electricity production.

Solar PV-based rural electrification architectures for DC microgrids typically proposed in the literature use

Manuscript received February 11, 2017; revised May 8, 2017 and July 12, 2017; accepted August 1, 2017. Date of publication August 4, 2017; date of current version December 14, 2017. This work was supported in part by the Faculty Initiative Funding grant from the Lahore University of Management Sciences. Paper no. TSTE-00134-2017. *(Corresponding Author: Mashood Nasir.)*

M. Nasir, A. Hussain, and L. Mateen are with the Department of Electrical Engineering, Lahore University of Management Sciences, Lahore 54792, Pakistan (e-mail: 14060018@lums.edu.pk; arif.hussain@lums.edu.pk; 15100082@lums.edu.pk).

H. A. Khan was with the School of Electrical Engineering, University of Manchester, Manchester M13 9PL, U.K. He is now with the Department of Electrical Engineering, Lahore University of Management Sciences, Lahore 54792, Pakistan (e-mail: hassan.khan@lums.edu.pk).

N. A. Zaffar was with the Electro-Optic/Magneto-Optic Labs, University of Pennsylvania,, Philadelphia, PA 19104 USA, and Techlogix Pakistan Pvt. Ltd., Lahore 54000, Pakistan. He is now with the Department of Electrical Engineering, Lahore University of Management Sciences, Lahore 54792, Pakistan (e-mail: nauman.zaffar@lums.edu.pk).

Color versions of one or more of the figures in this paper are available online at http://ieeexplore.ieee.org.

Digital Object Identifier 10.1109/TSTE.2017.2736160

1) Centrally located generation (referred to as "central generation") with centrally located battery storage (referred to as "central storage") [10]–[13].
2) Central generation with distributed storage [7], [14].

The central positioning of the resources is generally beneficial from the perspective of control, where overall generation and storage level (state of charge) are reliably monitored. However, this results in higher distribution losses and rigidity in terms of future expansions [15]. More critically, their field deployments at higher power loads are particularly difficult because of the high capital costs of sustaining a large system with central solar generation. One approach that stands out in this regard is "Mera Gao Power" (MGP) in India, which provides only 5 W of DC power to each subscribing house, with a limit of 0.2 amps—enough to power two LED lights and a mobile phone-charging point [12], [13]. The implementation involves central PV generation and central battery storage with distribution at 24 V of DC to subscribing houses. However, due to very limited power supply, such a scheme is unlikely to alleviate poverty in rural areas or contribute to significant improvements in their socio-economic circumstances [16]. If such a central generation central storage architecture (CGCSA) is implemented for high power loads for households (50 W or higher), the losses associated with the distribution of energy are significantly higher, thereby making the scheme unviable.

Another PV-based ad-hoc DC microgrid architecture for rural electrification proposed by Wardah *et al.* [17] integrates the power needed for several consumers (up to 20) into a single generator unit. However, the overall distribution is at 48 V, which renders it impractical for the requirements of larger households or a community level load due to higher distribution losses. Alternatively, for a higher voltage distribution of 380 V, Madduri *et al.* [7], [14] proposed a PV-based central generation and distributed storage architecture (CGDSA). The provision of energy storage at local houses results in higher efficiency than through CGCSA, but this architecture is still suboptimal in two respects: a) central PV generation requires a higher upfront cost because a large nameplate capacity is required for the solar panel at the outset, resulting in a cost barrier; and b) distribution to distant houses causes significant system losses. Several other studies [18]–[20] have proposed advancements in aspects of control related to DC microgrids through hierarchical, supervisory, and adaptive droop control schemes. These require extensive monitoring, sensing, and communication, which adds to the complexity and cost of the microgrid. From the perspective of rural electrification, a costly and complex system is unsuitable.

In light of the limitations on (a) distribution efficiency, (b) power supply for household-level loads, (c) provision of communal loads, (d) rigidity in future expansion, and (e) requirements for extensive control techniques in the above-mentioned architectures for a DC microgrid, we propose a solar PV-based scalable, distributed generation and distributed storage architecture (DGDSA) with a novel resource (power)-sharing provision among the distributed resources (see Fig. 1). The architecture has the built-in advantages of (a) higher efficiency because of distributed generation and distributed storage, (b) modular scalability for future expansion, (c) efficient aggregation of power for larger loads even with limited rooftop PV, (d) delivery to such communal entities as rural schools and basic health units by pooling power from individual household units without dedicated (large) generation, (e) reliable and simplified control through the hysteresis-based voltage droop method (implemented through a localized controller without the need for central, adaptive, or supervisory control, and a reduction in extensive communication requirements. Furthermore, the distributed nature of the proposed DGDSA makes it independently scalable in its planning and operation. To the best of our knowledge, none of the existing architectures provides this level of scalability because the requirements of these architectures for upfront generation are generally higher. For instance, the architecture developed by Madduri *et al.* [7], [14] features central generation, which requires a relatively larger generation capacity at the outset for village-scale electrification.

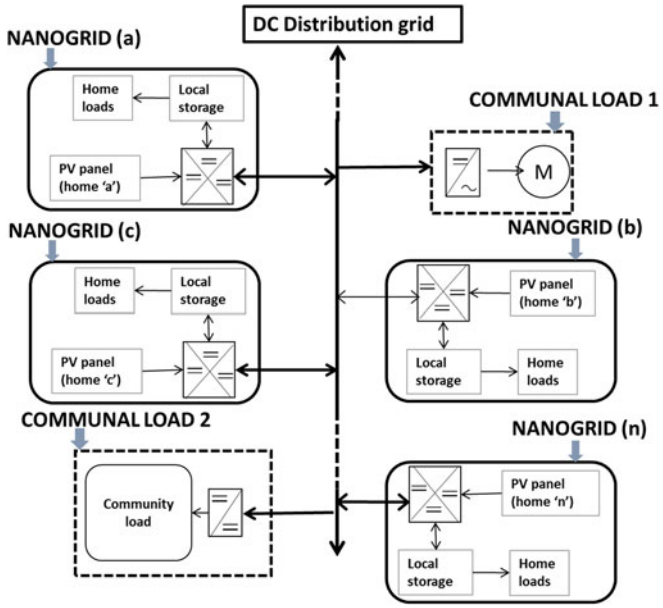

Fig. 1. Conceptual diagram of microgrid architecture with contributing nanogrids (households) and communal loads.

Similarly, the architecture proposed by Wardah *et al.* [17] has cluster-/neighborhood-level distributed generation to cater to the needs of multiple houses and, therefore, requires a larger number of subscribing houses for the system to be viable. Other architectures [12], [13] also use central generation requiring a certain minimum number of subscribers for proper utilization. On the contrary, in our proposed architecture, even a single system installed (panel, power processing unit, and battery) at a house can initiate the operation of the DGDSA-based DC microgrid, which can then grow in a scalable manner as neighbors are added to the grid.

In our earlier work, a comparative analysis of different architectures—the CGCSA, the CGDSA, and the proposed DGDSA—was carried out in terms of distribution efficiency by using the Newton–Raphson method modified for DC power [15]. The analysis in [15] showed that for all ranges of power provision, distribution voltage levels, and conductor sizes, the

TABLE I
COMPARISON AMONG DC MICROGRID ARCHITECTURES

Type of Microgrid	Maximum Distribution Efficiency (%)	Maximal Voltage Drop (%)	Architecture References
CGCSA	91.9	8.86	[10]–[13]
CGDSA	93.4	5.33	[7]–[14]
DGDSA	96.70	3.5	[15]

proposed DGDSA exhibits higher efficiency, lower line losses, and minimal voltage drops in comparison with the other architectures [15]. A summary of the distribution efficiencies and voltage drops is shown in Table I. In this study, we highlight the design of the DGDSA, which supports the provision of large amounts of power to households and communal loads using a scheme for the integration of the power electronic interface with the distributed resources in the microgrid. Resource sharing capability and a simplified distributed droop control, which are key enablers of scalability and the provision of large amounts of power, are analyzed for power sharing scenarios among the contributing nanogrids.

The rest of this paper is organized as follows: In Section II, the architecture of the proposed microgrid is presented in terms of the interconnection of contributing nanogrids. In Section III, the Newton–Raphson power flow analysis modified for the DGDSA-based DC microgrid is presented. The distributed voltage droop algorithm for the stable operation of the microgrid is formulated on the basis of the microgrid energy balance in Section IV. Section V presents simulations and results for power flows as well as the cost analysis of a sample system. Challenges to the practical deployment of the proposed architecture along with possible future enhancements are discussed in Section VI.

II. ARCHITECTURE OF THE PROPOSED DC MICROGRID

The electrical energy architecture proposed here is a distributed type of microgrid (Fig. 1)—a small, interconnected, self-sustaining electrical generation, distribution, and utilization system. A household is a basic building block referred to as a nanogrid. The primary task is to establish an efficient mechanism via PV-distributed generation (DG) to channel excess energy among the connected nodes.

For instance, in Fig. 1, PV panels at the rooftop (home "a") should be able to provide electricity to a neighboring house (home "b") if the PV-generated power is not being utilized in home "a," and vice versa. Similarly, if both home "a," home "b," up to home "n," have surplus power, a mechanism is needed to allow this power to be utilized for communal loads. Therefore, in a communal setting, the surplus DC power produced by all panels must also be utilizable for communal loads, such as water pumps for drinking/irrigation, lighting, and computing loads in schools. The supply of power for large communal loads is otherwise often expensive and unsustainable in the rural areas of developing countries.

A. Model of Nanogrid

A nanogrid is a basic building block of the microgrid architecture that integrates its resources in a scalable manner into the community. Each house contains a roof-mounted solar panel, a few DC loads and battery storage. The bidirectional flow of power is controlled via power electronic converters referred to as central power processing units (CPPUs). A CPPU contains a microcontroller along with a maximum power point tracking (MPPT)-based DC-DC converter and a bidirectional flyback converter.

1) DC–DC MPPT Converter: The output power of a PV panel is a non-linear function of temperature and incident irradiance [21]. MPPT techniques are employed to extract the maximum power from the available solar energy. Various schemes for MPPT under uniform and non-uniform irradiance have been discussed in the literature [22], [23]. In this article, the perturb and observe (P & O) algorithm is employed due to its simplicity and low computational complexity [22]. The conversion ratio of the DC-to-DC converter is adjusted such that its output voltage is suitable for supplying power to the load and charging the battery. Based on the time-varying values of the output voltage and current of the PV panel, the controller adjusts the duty cycle of the converter to obtain the desired voltage conversion or MPPT for all operating conditions.

2) Bidirectional Flyback Converter: A bidirectional flyback converter is employed to enable the resource sharing feature, as it allows for the transfer of power from nanogrids to the microgrid, and vice versa. Bidirectional power flow is attained through modified switch realization, i.e., by replacing the diode of a conventional flyback converter with another controlled MOSFET switch. The position of the switch is modified to ensure that the source is grounded without affecting the continuity of the circuit by mitigating the requirement for a complex bootstrapping circuit (see Fig. 3). A detailed performance analysis of the deployed bidirectional flyback is provided in [24].

A flyback converter has the advantages of simpler design and lower cost (the use of fewer components) than other types of buck–boost converters; therefore, it is suitable for DC microgrid applications [25]. Along with the higher conversion ratio, it allows for the use of the inherent magnetizing inductance of the flyback transformer, thus eliminating the need for an extra inductor to transform the energy of the converter. The implementation of the bidirectional switch of the flyback converter is shown in Fig. 3. The governing equation of the continuous conduction mode (CCM) for voltage conversion gain *M(d)* in terms of the transformer's turn ratio *N*, and the battery voltage $V^B(t)$ and the duty cycle *d* of the converter at any time *t* is

$$M(d) = \frac{V^B(t)}{V^G_{\text{rated}}} = N\frac{d(t)}{1-d(t)} \tag{1}$$

B. Model of a Village and Microgrid Scheme of Interconnection

Depending upon the structure, a typical village containing *n* houses is divided into *x* segments with *n/x* houses per segment, as shown in Fig. 2. The structure of a nanogrid is shown in

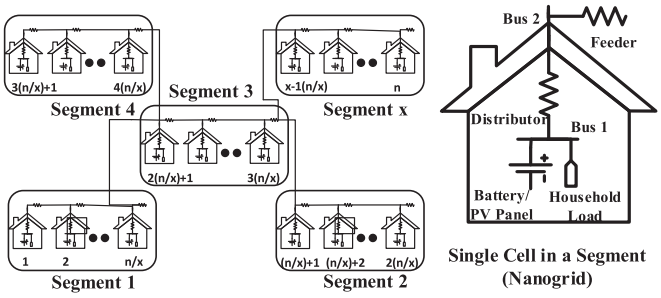

(a)

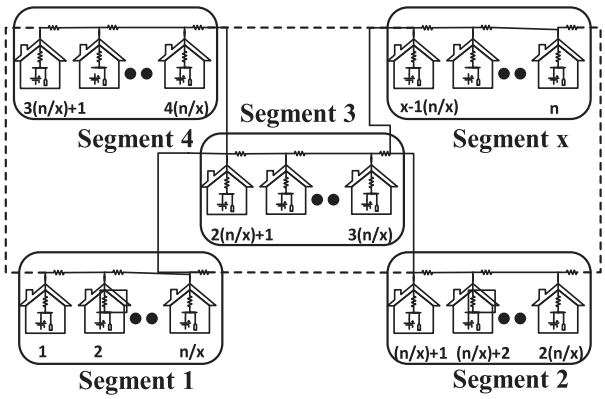

(b)

Fig. 2. (a) Proposed architecture of the radial schemes of interconnection with elaborated single-unit design. (b) Proposed architecture of the ring main schemes of interconnection.

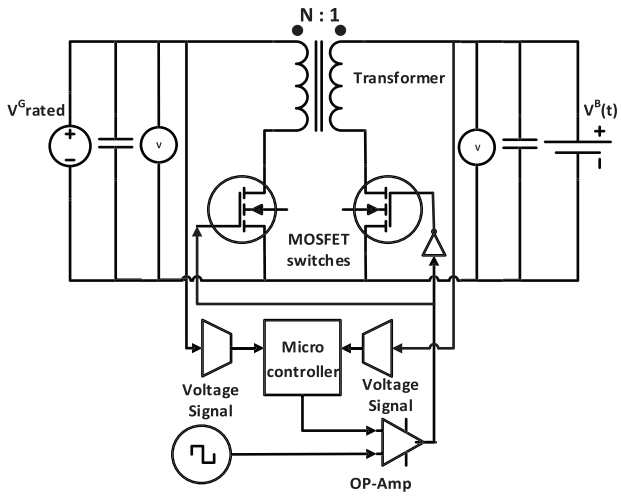

Fig. 3. The implementation of the bidirectional switch and the control of the flyback converter.

Fig. 2 (a). Power is supplied to the load in each household via a flyback converter that, along with the resistance of the supplying wire, is modeled as a constant power bus and represented by a distributor resistance (Fig. 2 (a)). The interconnection resistance between two consecutive nanogrids is modeled as feeder resistance.

Two interconnection schemes are considered and shown in Fig. 2. Fig. 2 (a) shows the radial interconnection of nanogrids that lowers the cost of the conductor in the system design. However uneven loading, non-uniform voltage distribution, high-voltage dips at the rear end, and subsequent reliability issues render radial schemes a relatively poor choice for the optimal distribution of power [26], [27]. Therefore, to address these issues, the ring main scheme of interconnection is proposed (Fig. 2 (b)). It uses an extra layer of conductors (dashed lines) to connect feeders at the periphery of radial architecture in a ring main fashion. Thus, at the cost of extra conductors, higher efficiency and increased reliability are achieved, even at comparatively low distribution voltages.

Using the values of the feeder and the distributor resistances, based on the scheme of the interconnection and topological configuration of a village, a conductance matrix *G* can be calculated to model it. For a village with *n* houses, *G* is of the order of $2n \times 2n$, as each house contains two buses: 1) a load bus at the interconnection of the distributor resistance and the load bus, and 2) another bus at the interconnection of the feeder and the distributor resistances (Fig. 2). Thus, elements of the conductance matrices G_{ij} and *G* can be written in terms of individual conductance g_{ij} between any arbitrary buses *i* and *j*, where *i* may vary from 1 to *2n*:

$$G_{ij} = \begin{cases} \sum_{\substack{j=1 \\ j\neq i}}^{2n} g_{ij}; \forall \mathrm{i} = j \\ -g_{ij}; \qquad \forall\, \mathrm{i} \neq \mathrm{j} \end{cases} \tag{2}$$

$$G = \begin{bmatrix} G_{11} & \mathrm{G}_{12} & \cdots\cdots & \mathrm{G}_{1,2n} \\ G_{21} & \mathrm{G}_{22} & \cdots\cdots & \mathrm{G}_{2,2n} \\ \vdots & \vdots & \ddots & \vdots \\ G_{2n,1} & \mathrm{G}_{2n,2} & \cdots\cdots & \mathrm{G}_{2n,2n} \end{bmatrix}; G \in R^{2n\times 2n} \tag{3}$$

III. Power Flow Analysis for Optimal Selection of Voltage Level and Conductor Size

Power flow analysis was conducted using the Newton–Raphson method modified for our DC microgrid [15]. This was necessary to ascertain various critical elements of the proposed system, particularly total line losses, efficiency, and voltage drops. These parameters were used as an indicator for the selection of the optimal voltage for the DC microgrid. Depending on the load requirements, load is scheduled on each bus *i* and the scheduled load matrix P^{sch} is given by (4):

$$P_{\mathrm{sch}} = \left[P_1^{\mathrm{sch}}\, P_2^{\mathrm{sch}}\, P_3^{\mathrm{sch}} \cdots\cdots P_{2n}^{\mathrm{sch}}\right]^t; P_{\mathrm{sch}} \in R^{2n\times 1} \tag{4}$$

Based on the conductance matrix model of the village, instantaneous power at the ith bus P_i^{cal} can be calculated by (5):

$$P_i{}^{cal} = V_i I_i = \sum_{j=1}^{2n} V_i V_j G_{ij} \tag{5}$$

Therefore, the load matrix P^{cal} is given by (6):

$$P^{cal} = \left[P_1^{cal}\, P_2^{cal}\, P_3^{cal} .....P_{2n}^{cal}\right]^t; P^{cal} \in R^{2n*1} \tag{6}$$

Subtracting (4) from (6) while expanding the remaining terms using the Taylor series (neglecting higher-order terms)

gives (7) [28]:

$$\begin{bmatrix} \Delta P_2{}^{(k)} \\ \vdots \\ \Delta P_{2n}{}^{(k)} \end{bmatrix} = \begin{bmatrix} \dfrac{\partial P_2{}^{(k)}}{\partial V_2} & \cdots & \dfrac{\partial P_2{}^{(k)}}{\partial V_{2n}} \\ \vdots & & \vdots \\ \dfrac{\partial P_{2n}{}^{(k)}}{\partial V_2} & \cdots & \dfrac{\partial P_{2n}{}^{(k)}}{\partial V_{2n}} \end{bmatrix} \begin{bmatrix} \Delta V_2{}^{(k)} \\ \vdots \\ \Delta V_{2n}{}^{(k)} \end{bmatrix} \quad (7)$$

where, $\Delta P_i^{(k)}$ is the difference between the scheduled powers P_i^{sch} and P_i^{cal} on bus *i* at the kth iteration, and V_{rated}^G is the reference voltage. Using (7), the change in the voltages ΔV and the corresponding bus voltage V_i over *k* iterations are calculated until the difference between the scheduled and the calculated power becomes negligible. By using the convergent value of the voltage at each bus, the associated line losses LL_g, the percentage line losses $\%LL_g$, the percentage voltage drop $\%VD_g$, and efficiency η_g of the DC microgrid are calculated using (8) to (11), respectively:

$$LL_g = \frac{1}{2}\sum_{i=1}^{2n}\sum_{j=1}^{2n} G_{ij}\left(V_i\left(V_i - V_j\right) + V_j\left(V_j - V_i\right)\right) \quad (8)$$

$$\%LL_g = \frac{LL_g}{P_G} * 100\%, \text{ and } P_G = \sum_{i=1}^{n}\left(P_i > 0\right) \quad (9)$$

$$\eta_g = 100 - \%LL_g \quad (10)$$

$$\%VD_g = \frac{V_i^{\max} - V_i^{\min}}{V_i^{\max}} * 100\% \quad (11)$$

where, $V_i^{\max}$ and $V_i^{\min}$ are the maximum and minimum values of the voltage at any bus after the kth iteration, respectively. From (6)–(11), it is clear that line losses, efficiency, and voltage drops in the microgrid system are a function of rated grid voltage V_{rated}^G and conductance matrix G_{ij}. Therefore, by using the above analysis, optimal distribution voltage and optimal conductor size may be selected for the DGDSA-based electrification of a village depending on the number of households, power provided to an individual household, allowable power sharing among houses, and the scheme of interconnection.

IV. Hysteretic Voltage Droop Algorithm for Distributed Control of DGDSA

Energy balance for an ideal DGDSA-based village (Fig. 2) containing *n* households with distributed PV generation P_i^{PV} *(t)* at any time *t* is given by (12), based upon the constraints given in (13):

$$\sum_{i=1}^{n} P_i^{PV}(t)\Delta t = \sum_{i=1}^{n} P_i^{L}(t)\Delta t + \sum_{i=1}^{n} V_i^{B}(t)\Delta SOC(t) \quad (12)$$

$$P^{PV}, P^{L}, V^{B}, \Delta SOC \in R^{n\times 1}$$

$$\Delta SOC_i^{\min} \le \Delta SOC_i \le \Delta SOC_i^{\min}; \forall t \quad (13)$$

where, $V_i^B(t)$ is the household battery voltage, *SOC* is the state-of-charge of the battery, $SOC_i{}^{\max}(t)$ and $SOC_i{}^{\min}(t)$ are the allowable limits on the battery's SOC, and $P_i^L(t)$ is the household load power connected to the battery bus drawing $I_i(t)^L$ for any time interval Δt. For the grid to operate at rated voltage V_{rated}^G with net current $I^G(t)$, the batteries can either deliver power to the grid or take power from it using the bidirectional flyback converter. Therefore, (12) can be written in terms of battery current $I_i^B(t)$, which may have either a positive or a negative value depending on the state of the grid and subject to the constraints in (15):

$$\sum_{i=1}^{n} V_{\text{rated}}^G I_i^G(t)\Delta t = \sum_{i=1}^{n} V_i^B I_i^L(t).\Delta t + \sum_{i=1}^{n} V_i^B I_i^B(t)\Delta t \quad (14)$$

$$0 \le I_i^L \le I_i^{L,\max}, -I_i^{B,\min} \le I_i^B \le I_i^{B,\max}; \forall t \quad (15)$$

where, $I_i^{L,\max}$ is the maximum value of the permissible load current at each house, and $I_i^{B,\max}$ and $I_i^{B,\min}$ are the limits on the charging and discharging currents of the battery.

Based on the duty cycle control of the flyback converter, power may be channeled from the microgrid to nanogrid or vice versa. If the flyback converter operates at critical duty d_i^{cric} (given by (16)), there is zero power sharing between the microgrid and the battery of household *i*. To set the direction and magnitude of power flow from microgrid to nanogrid, a positive perturbation in duty Δd_i is applied. Thus, the flyback converter channels the power from the microgrid to the load bus when operating above critical duty $d_i^{\text{cric}} + \Delta d_i$. Below the critical duty $d_i^{\text{cric}} - \Delta d_i$, the bidirectional flyback converter ensures the flow of power from battery to microgrid. Thus, the energy stored in the battery may be transferred back to the grid using the negative perturbation in critical duty.

$$d_i^{\text{cric}}(t) = \frac{V_i^B(t)}{V_i^B(t) + NV_{\text{rated}}^G} \quad (16)$$

For stable microgrid operation, the duty of each flyback converter is adjusted such that it produces V_{rated}^G at the microgrid; therefore, using (1), (14) may be written as follows, subject to the constraints in (15):

$$\sum_{i=1}^{n} I_i^G(t) = N\sum_{i=1}^{n} \frac{d_i(t)}{[1-d_i(t)]}\left(I_i^L(t) + I_i^B(t)\right) \quad (17)$$

The stable operation of the microgrid is defined by the hysteresis in grid voltage such that $V_{\text{min}}^G \le V_{\text{rated}}^G \le V_{\text{max}}^G$, where, V_{min}^G and V_{max}^G are the minimum and maximum values of the grid voltage, respectively, dictated by the hysteresis generally maintained at $\pm 2\%$ of the rated grid voltage. Using the power balance of (17), an algorithm is formulated (shown in Fig. 4) for generalized microgrid operation based on the duty cycle control of the flyback converter of each household. The perturbation applied in the duty cycle adjusts the direction and amount of allowable power shared between the nanogrids and the microgrid, hence maintaining power flow such that the microgrid is always stable.

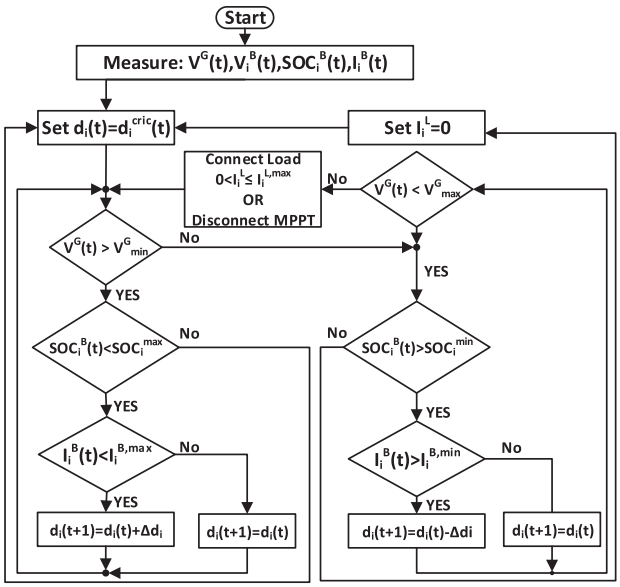

Fig. 4. Hysteretic-based distributed voltage droop control algorithm.

As an example, if the grid has excess power available, the positive perturbation channelizes the excess power toward the battery storage of the nanogrid or as an elastic load. In this situation, the voltage of the microgrid decreases in proportion to the net power transfer. Our algorithm ensures that if the grid voltage drops below $V^G_{\min}$, the direction of power flow is reversed using a negative perturbation in the duty of the flyback converter to maintain balance in voltage. Thus, a negative perturbation applied above the critical duty channelizes the stored power of the battery toward the microgrid to increase its voltage above $V^G_{\min}$ to $V^G_{\max}$. Thus, hysteresis-based voltage droop control determines the required perturbation in the duty and the associated amount of power flow between microgrid and nanogrid while keeping the voltage within the hysteretic limit, hence ensuring the stability of the scheme throughout its operation. Because of this distributed control structure, each nanogrid is responsible for the stable operation of the microgrid. Therefore, the need for a central controller and a costly communication interface is obviated in the proposed architecture. Further, the hysteresis-based voltage droop control also renders the proposed DGDSA highly scalable in terms of future expansions.

V. Results and Discussion

To test the proposed methodology, a typical village of a developing country consisting of 40 houses was considered. Each house had a PV generation capacity of 250 W_P (the maximum power at standard input irradiance of 1000 W/m^2), a battery with a storage capacity of 100 Ah (lead acid), and was capable of driving rated 40 W of DC load including lighting, fan, and charging. The village was distributed into five segments with eight houses per segment. The distance between consecutive houses (feeder) and the length of the internal wiring (distributor) was 20 m, consistent with the situation in rural settlements in developing countries as described by Varshney *et al.* [29].

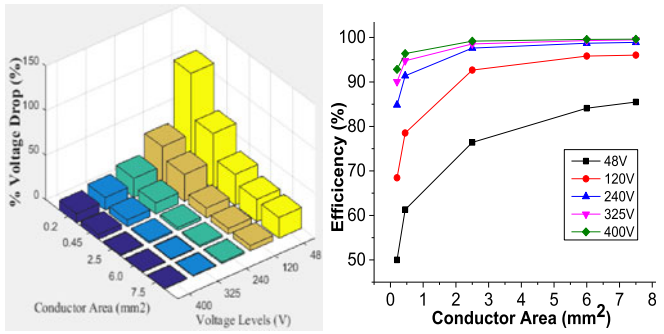

Fig. 5. Percentage voltage drop and efficiency at different voltages and conductor sizes at peak load sharing on the radial scheme.

A. Simulation Results of Power Flow Analysis for the Selection of Optimal Voltage Level, Conductor Size, and Interconnection Scheme

The selection of the optimum distribution voltage is a critical aspect of the microgrid as it influences the operation, control, protection, and safety aspects [26], [28]. Viable levels of LVDC, i.e., 48 V, 120 V, 230 V, 325 V, and 400 V, were considered for analysis. Conductors with wire gauge areas of 0.2 mm^2 (local market name 3.0-0.029"), 0.45 mm^2 (local market name 7.0-0.029"), 2.5 mm^2, 6 mm^2, and 7.5 mm^2 were used. Using (2)–(11), a program was written on MATLAB to calculate percentage line losses, percentage voltage drop, and efficiency for both schemes of interconnection to select the optimal voltage level and conductor size.

1) DGDSA With Radial Scheme of Interconnection: Typical and peak load scenarios were studied for the DGDSA with the radial scheme of interconnection. In a typical load scenario, power sharing between houses and the grid is taken to be $\pm 20\%$ (a house can demand 20% more or supply 20% of its rated power). Since power sharing was kept limited, with the average conductor size (2.5 mm^2), distribution losses and percentage voltage drops were low at 120 V and higher voltages, with efficiency values above 99%.

The situation changed significantly when the power sharing provision was increased, i.e., $\pm 100\%$. Under the peak load sharing scenario, a house could consume twice its rated power and supply all its available power to the grid. The results showed that efficiency was lower at low voltages, and a significantly higher cost of a thick conductor was incurred for this topology, as shown in Fig. 5.

2) DGDSA With Ring Main Scheme of Interconnection: The ring main topology significantly improves efficiency at peak load sharing in comparison with radial topology. It also provides the necessary redundancy to ensure service operation in case of grid disconnection due to a fault or severed wires. The results for peak load sharing on the ring main scheme are shown in Fig. 6. From a comparison of Figs. 5 and 6, it is evident that the ring main topology had higher efficiency and fewer voltage drops in comparison with the radial scheme. For instance, in case of peak load sharing at 120 V using a conductor with an area of 2.5 mm^2, the ring main scheme yielded higher ef-

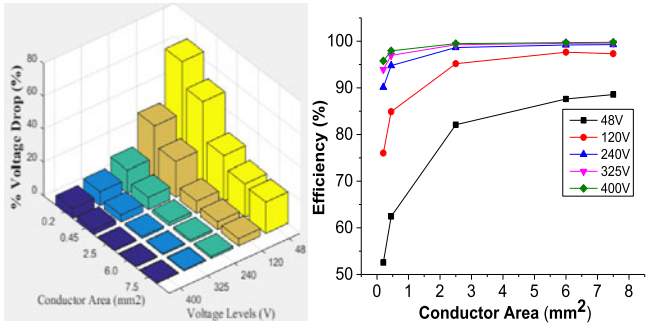

Fig. 6. Percentage voltage drop and efficiency at different voltages and conductor sizes for peak load sharing on the ring main scheme.

TABLE II
PEAK LOAD COMPARISON BETWEEN RADIAL AND RING MAIN DGDSA

Distribution Voltage (V)	Conductor Area (mm^2)	Radial Microgrid			Ring main Microgrid		
		LL_g (%)	VD_g (%)	η (%)	LL_g (%)	VD_g (%)	η (%)
48	2.5	23.5	34.4	76.41	17.9	27.1	82.1
120	2.5	7.34	10.9	92.66	4.82	7.38	95.18
400	2.5	0.83	1.23	99.17	0.51	0.77	99.49

ficiency (95.18%) than the radial scheme (92.66%). In other configurations, where the cost of an end-to-end ring conductor is much higher than the respective gains in efficiencies, the radial scheme was the simplest choice available.

Table II shows that upon increasing the voltage from 48 V to 120 V, there was a significant increase in the distribution efficiency. Up to 120 V, the associated protection and safety requirements were not excessive [30], [31]. Moreover, voltages lower than 120 V were considered safe for indirect touch, and required no extra grounding and protective conductors [30]. However, moving from 120 V to 400 V, the percentage reduction in losses was lower but the system's complexity, and safety requirements increased significantly. Voltage levels lower than 48 V were unsuitable for distribution as the voltage drop was considerably higher than 15%. Distribution at 120 V was generally less efficient than at 400 V; however, the ring main interconnection between feeders largely mitigated this loss at the cost of extra conductors and added the necessary redundancy for reliable operation.

The analysis showed that for the selected parameters, the distribution losses were less than 3% even at a communal load of 400 W. Therefore, for the considered specifications of the village, 120 V using a conductor of area 2.5 mm^2 and the ring main scheme of interconnection is optimum for the operation of the microgrid. For different load specifications for other villages, the proposed analysis may yield optimum voltage levels others than 120 V, depending on the trade-off between losses and the cost of the protective equipment.

B. Analysis of Levelized Cost of Electricity

Based on information pertaining to the selected voltage level (as converter specifications in CPPU depend on the voltage level), conductor size, the PV panel, and battery size, a cost analysis was conducted to evaluate the financial viability of the proposed system. The system specifications—various components of cost in the implementation of the proposed system, along with the results of cost analysis, including upfront cost, lifecycle cost, and the levelized cost of electricity (LCOE)—are highlighted in Table III. The model for estimating the cost of various components of the system, including the cost/W_p of the PV panel, the distribution conductor, and protection, were taken from [14]. However, the costs of the battery and the converter were fundamentally different from those in [14] because of difference in the deployed battery technology (lead acid instead of Li-ion), architecture, and the distribution voltage level. The LCOE calculated for the proposed architecture over a horizon of 25 years was \$0.099/kWh, significantly lower than that in [14] because of reduced panel and battery sizes. The proposed DGDDSA can extract the benefit of usage diversity and, therefore, ensures optimal resource utilization.

TABLE III
COST ANALYSIS OF PROPOSED DGDSA-BASED DC MICROGRID

System Parameters	
Length of Microgrid	800 m
No. of households	40
Rated energy usage of each household	960 Wh
Rated power of communal load	400 W
Household operation	24 h
Communal load operation	6 h
PV panel rating at each household	250 W_p
Battery rating at each household	1.2 kWh
Upfront System Cost Parameters	
PV generation cost	\$7000
Battery Storage cost	\$3600
CPPU cost	\$2000
Conductor and protection cost	\$4000
Upfront cost	\$16600
System Cost Parameters for 25-year Life	
Number of battery replacements	4
Number of CPPU replacements	2
Miscellaneous Costs	\$2000
Cot of 25-year system life	\$37000
Number of Units Produced over Lifetime	372.3 MWh
Levelized cost of electricity (LCOE)	\$0.099/kWh

C. Scaled-Down Hardware Implementation for DC Power Flow Analysis

The proposed model that originally contained 40 houses was scaled down to three houses for practical implementation, where each house could either generate or consume 40 W of power under various scenarios. The generation capacity of each house was implemented via power supplies (ESCORT EPS3030T) and consumption capability through DC load banks (LABTECH LEMSPL) available in the laboratory [32], [33]. Both the radial and the ring main scenarios were tested for line losses, efficiency, and voltage dips. The results were in agreement with the simulation outcomes as shown in Fig. 7.

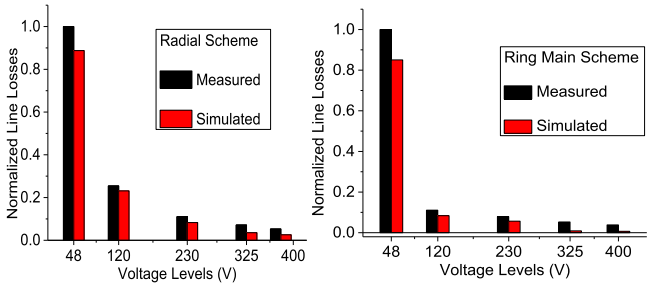

Fig. 7. Simulated versus measured results for normalized line losses in the DGDSA using the radial and the ring main schemes of interconnection.

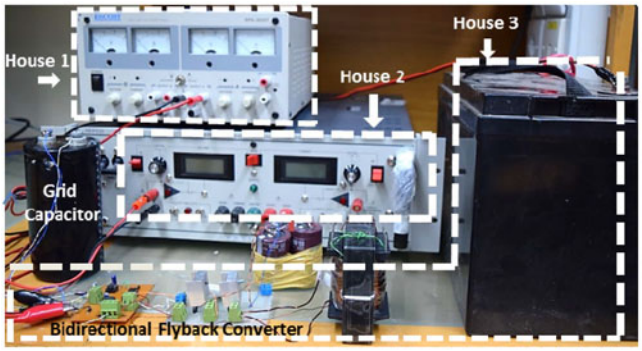

Fig. 8. Implementation of the DGDSA microgrid hardware through the integrations of nanogrids.

D. Hardware Implementation of Power Electronic Interface for DGDSA-Based Integration of Nanogrids into Microogrid

The distribution voltage of the grid V^G_{rated} was 120 V while the house load distribution and storage voltage V^B was 12 V. The setup for the integration of three atomic nanogrids into into the microgrid is shown in Fig. 8. The DC microgrid was implemented using a large capacitor (5000 μF), the states of charging and discharging of which were continuously monitored. House 1 (H1) supplied constant power, and was modeled using a DC power supply (ESCORT EPS3030T) [33]. House 2 (H2) was modeled using a four-quadrant bipolar power supply that could act as a power source or sink [34]. House 3 (H3) was modeled using by a battery along with a bidirectional flyback converter.

Typical voltage variations of the microgrid in various power sharing scenarios are shown region wise in Fig. 9. In "Region 1," houses 2 and house 3 used power from the grid while house 1 supplied to it. Based on the algorithm in Section IV, when the power supplied by house 1 was less than the power being taken by the other two houses, the voltage of the grid decreased. As the voltage dropped below the specified lower threshold $V^G_{\text{min}} = 117.5$ V, the loads of both houses were turned off. In "Region 2," power from the battery bank in house 3, house 1, and house 2 started charging the grid again to increase its voltage above 120 V. When the voltage was above the hysteretic threshold of the grid, set to 122.5 V, the loads were turned on again per the proposed algorithm. In "Region 3," houses 1 and 2 supplied power to charge the battery of house 3. The battery voltage "V^B" is also constantly monitored during charging and discharging as shown in Fig. 9. The state of the system was not kept fixed at

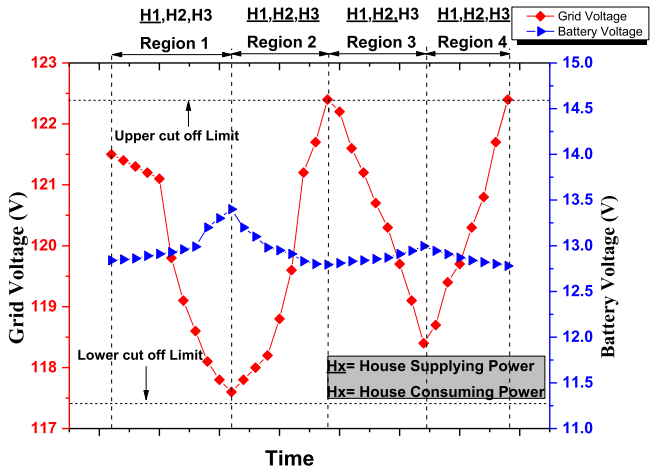

Fig. 9. The results of hardware implementation of typical voltage variations of the microgrid in various power sharing scenarios.

120 V; rather, hysteresis was kept at around the upper and lower cut-off limits, i.e., $V^G_{\text{max}} = 122.5$ and $V^G_{\text{min}} = 117.5$ V. Therefore, a balanced load and bidirectional flow of power were maintained throughout the operation to ensure the stability of the grid.

VI. Challenges to Practical Deployment of the Proposed Architecture

Although the proposed architecture allows for the efficient utilization of distributed resources in a highly scalable manner, some challenges associated with larger deployments persist. High-level distribution of resources poses a challenge with respect to safety and protection due to the increased likelihood of short circuit contribution from multiple paths within the microgrid. Therefore, future large-scale practical implementations must include an intelligent protection scheme capable of real-time load flow and short circuit analysis for adaptive relay settings (not part of the scope of this study). Further work on the islanded operation of the microgrid is also important to ensure optimum isolation from the grid for enhanced safety. From the perspective of control, although hysteretic-based voltage droop control can reduce multiple layers of sensing and control in the DGDSA, for large-scale implementations, additional sensing and hierarchical control layers may be added to ensure the enhanced stability of the microgrid over a wide range of operations.

Another important aspect that needs to be addressed in future work is the selection of the optimal size of various components of the architecture, mainly included PV generation capacity, battery storage capacity, and conductor size, based on the region-specific profiles of temperature and incident irradiance. In our view, detailed region-specific profiling can be crucial to ensuring optimal planning and efficient resource utilization in such electrification architectures, reducing the LCOE further for many deployments.

From the perspective of the financing of rural microgrids, the role of micro-financing institutes is critical [35]. Technical innovations must be coupled with suitable business models to ensure wide uptake of energy-related initiatives. The participation of

the private sector has grown in recent years [36] but more needs to be done. For instance, experience of past rural electrification projects in South Asia suggests subsidized micro-financing schemes for local communities along with public/private partnerships for the successful implementation of such projects [37], [38].

VII. Conclusion

This paper proposed an optimized DC microgrid architecture for rural electrification with emphasis on the providing power for purposes beyond those related to subsistence-level living. The results of analyses show that the proposed distributed storage architecture can enhance distribution efficiency by approximately 5% more than other LVDC architectures. Moreover, the proposed DGDSA is scalable in terms of its design and operation. These gains in terms of efficiency and scalability are achieved through a modular interconnection of various contributing households (nanogrids) with distributed control attained through the hysteretic voltage droop method. This distributed solar PV generation and storage allows power sharing conducive to larger communal loads unavailable in other architectures. For a typical village arrangement in a developing region with 40 households, a distribution efficiency of 96% can be achieved for a typical 2.5-mm^2 conductor, even at a low distribution voltage of 120 V DC (ring main topology) with peak load sharing capability. The proposed architecture is therefore ideal for rural electrification in developing countries.

References

[1] R. Singh and K. Shenai, "DC microgrids and the virtues of local electricity," *IEEE Spectrum*, vol. 51, no. 2, Feb. 2014.

[2] World Energy Outlook (WEO, 2016), Electricity Access. [Online]. Available: http://www.worldenergyoutlook.org/resources/energydevelopment/energyaccessdatabase/

[3] M. N. Qaiser, M. Usama, B. Ahmad, M. A. Tariq, and H. A. Khan, "Low cost, robust and efficient implementation of MPPT based buck-boost converter for off-grid PV applications," presented at the *40th Int. Conf. IEEE Photovolt. Spec.*, Denver, CO, USA, 2014.

[4] H. A. Khan and S. Pervaiz, "Technological review on solar PV in Pakistan: Scope, practices and recommendations for optimized system design," *Renew. Sustain. Energy Rev.*, vol. 23, pp. 147–154, 2013.

[5] S. H. I. Jaffery *et al.*, "The potential of solar powered transportation and the case for solar powered railway in Pakistan," *Renew. Sustain. Energy Rev.*, vol. 39, pp. 270–276, 2014.

[6] J. Khan and M. H. Arsalan, "Solar power technologies for sustainable electricity generation–A review," *Renew. Sustain. Energy Rev.*, vol. 55, pp. 414–425, 2016.

[7] P. A. Madduri, J. Rosa, S. R. Sanders, E. A. Brewer, and M. Podolsky, "Design and verification of smart and scalable DC microgrids for emerging regions," in *Proc. 2013 Int. Conf. IEEE Energy Convers. Congr. Expo.*, 2013, pp. 73–79.

[8] D. Soto and V. Modi, "Simulations of efficiency improvements using measured microgrid data," in *Proc. 2012 Int. Conf. IEEE Glob. Humanitarian Technol.*, 2012, pp. 369–374.

[9] J. J. Justo, F. Mwasilu, J. Lee, and J.-W. Jung, "AC-microgrids versus DC-microgrids with distributed energy resources: A review," *Renew. Sustain. Energy Rev.*, vol. 24, pp. 387–405, 2013.

[10] S. Balijepalli, V. S. K. M. Khaparde, and S. A. Dobariya, "Deployment of microgrids in India," in *Proc. IEEE Power Energy Soc. Gen. Meet.*, 2010, pp. 1–7.

[11] P. Loomba, S. Asgotraa, and R. Podmore, "DC solar microgrids—A successful technology for rural sustainable development," in *Proc. 2016 Int. Conf. IEEE PES PowerAfrica*, 2016, pp. 204–208.

[12] D. Palit, G. K. Sarangi, and P. Krithika, "Energising rural India using distributed generation: The case of solar mini-grids in Chhattisgarh State, India," in *Mini-Grids for Rural Electrification of Developing Countries*, New York, NY, USA: Springer, 2014, pp. 313–342.

[13] D. Palit and G. K. Sarangi, "Renewable energy based mini-grids for enhancing electricity access: Experiences and lessons from India," in *Proc. Int. Conf. Utility Exhib. Green Energy Sustain. Develop.,* Mar. 2014, pp. 1–8.

[14] P. A. Madduri, J. Poon, J. Rosa, M. Podolsky, E. Brewer, and S. R. Sanders, "Scalable DC microgrids for rural electrification in emerging regions," *IEEE J. Emerg. Sel. Topics Power Electron.*, vol. 4, no. 4, pp. 1195–1205, Dec. 2016.

[15] M. Nasir, N. A. Zaffar, and H. A. Khan, "Analysis on central and distributed architectures of solar powered DC microgrids," in *Proc. 2016 Int. Conf. Clemson Univ. Power Syst.*, 2016, pp. 1–6.

[16] F. Pearce, "World's poor need grid power, not just solar panels. Energy and Fuels 2980," New Scientist, 2014.

[17] W. Inam, D. Strawser, K. K. Afridi, R. J. Ram, and D. J. Perreault, "Architecture and system analysis of microgrids with peer-to-peer electricity sharing to create a marketplace which enables energy access," in *Proc. 2015 9th Int. Conf. Power Electron. ECCE Asia*, 2015, pp. 464–469.

[18] J. Chi, W. Peng, X. Jianfang, T. Yi, and C. Fook Hoong, "Implementation of hierarchical control in DC microgrids," *IEEE Trans. Ind. Electron.*, vol. 61, no. 8, pp. 4032–4042, Aug. 2014.

[19] T. Vandoorn, J. De Kooning, B. Meersman, and L. Vandevelde, "Review of primary control strategies for islanded microgrids with power-electronic interfaces," *Renew. Sustain. Energy Rev.*, vol. 19, pp. 613–628, 2013.

[20] T. Dragičević, J. M. Guerrero, J. C. Vasquez, and D. Škrlec, "Supervisory control of an adaptive-droop regulated DC microgrid with battery management capability," *IEEE Trans. Power Electron.*, vol. 29, no. 2, pp. 695–706, Feb. 2014.

[21] C. S. Solanki, *Solar Photovoltaics: Fundamentals, Technologies and Applications*. New Delhi, India: PHI Learning, 2011.

[22] B. Subudhi and R. Pradhan, "A comparative study on maximum power point tracking techniques for photovoltaic power systems," *IEEE Trans. Sustain. Energy*, vol. 4, pp. 89–98, 2013.

[23] M. Nasir and M. F. Zia, "Global maximum power point tracking algorithm for photovoltaic systems under partial shading conditions," in *Proc. 2014 16th Int. Conf. Power Electron. Motion Control*, 2014, pp. 667–672.

[24] P. Thummala, Z. Zhang, and M. A. Andersen, "High voltage bi-directional flyback converter for capacitive actuator," in *Proc. 2013 15th Eur. Conf. Power Electron. Appl.*, 2013, pp. 1–10.

[25] R. Pasonen, "Model of Bi-directional flyback converter for hybrid AC/DC distribution system," *Int. J. Power Electron. Drive Syst.*, vol. 3, pp. 444–449, 2013.

[26] H. Saadat, *Power System Analysis*. New York, NY, USA: McGraw-Hill, 1999.

[27] V. Mehta and R. Mehta, *Principles of Power System*. New Delhi, India: S. Chand Publisher, 1982.

[28] J. D. Glover, M. S. Sarma, and T. J. Overbye, *Power System Analysis and Design*. Beijing, China: China Machine Press, 2004.

[29] K. R. Varshney *et al.*, "Targeting villages for rural development using satellite image analysis," *Big Data*, vol. 3, pp. 41–53, 2015.

[30] I. Marx, "Combining the best of both worlds," *IEEE Ind. Appl. Mag.*, vol. 16, no. 3, pp. 30–34, May-Jun. 2010.

[31] A. F. X. Welsch, "DC installation, different hazards regarding thermal effects and electrical shock," IEC/DKE LVDC Workshop, Regensburg Univ., Regensburg, Germany, 2011. [Online]. Available: workspaces.nema.org/public/LVDC/Lists/.../Attachments/5/1-2-LVDC_installation.pdf

[32] LABTECH (LEMSPL). [Online]. Available: http://www.eepowersolutions.com/products/portable-dc-load-banks-with-monitoring/

[33] EPS- 6030T. [Online]. Available: http://www.wavecom.com.au/04_product_documents/688/Brochure_EPS_6030T%20Power%20Supply_Ver_0.pdf

[34] KEPCO BOP 2001-D KEPCO, Inc. [Online]. Available: http://www.kepcopower.com/bop.htm

[35] S. C. Bhattacharyya, "Financing energy access and off-grid electrification: A review of status, options and challenges," *Renew. Sustain. Energy Rev.*, vol. 20, pp. 462–472, 2013.

[36] N. J. Williams, P. Jaramillo, J. Taneja, and T. S. Ustun, "Enabling private sector investment in microgrid-based rural electrification in developing countries: A review," *Renew. Sustain. Energy Rev.*, vol. 52, pp. 1268–1281, 2015.

[37] D. Palit, "Solar energy programs for rural electrification: Experiences and lessons from South Asia," *Energy Sustain. Dev.*, vol. 17, pp. 270–279, 2013.

[38] A. Newcombe and E. K. Ackom, "Sustainable solar home systems model: Applying lessons from Bangladesh to Myanmar's rural poor," *Energy Sustain. Dev.*, vol. 38, pp. 21–33, 2017.

Mashood Nasir received the B.S. degree in electrical engineering from the University of Engineering and Technology, Lahore, Pakistan, and the M.S. degree in electrical engineering from the University of Management and Technology (UMT), Lahore, in 2009 and 2011, respectively. He is currently working toward the Ph.D. degree in the Department of Electrical Engineering, Lahore University of Management Sciences, Lahore. From 2011 to 2012, he served as a Lecturer and during 2013–2014 he served as an Assistant Professor in Department of Electrical Engineering, UMT, Lahore. His research interests mainly include power electronics, electrical machines and drives, grid integration of alternate energy resources, electrochemical energy conversion and battery storage systems, and ac/dc/hybrid microgrids.

Hassan Abbas Khan (S'07–M'11) received the B.Eng. degree in electronic engineering from Ghulam Ishaq Khan Institute of Engineering Sciences and Technology, Topi, Pakistan in 2005. From 2005 to 2010, he was with the School of Electrical Engineering, University of Manchester, Manchester, U.K., where he first received the M.Sc. (with distinction) degree and then the Ph.D. degree in electrical and electronic engineering. He is currently serving as an Assistant Professor in the Department of Electrical Engineering, Lahore University of Management Sciences, Lahore, Pakistan. His current research interests include renewable energy and its uptake in developing countries. His core focus is on novel grid architectures for low-cost rural electrification through solar energy. He is also working on efficient and reliable solar PV deployments in urban settings to maximize their performance ratios.

Arif Hussain received the B.S. degree in electrical engineering from Lahore University of Management Sciences (LUMS), Lahore, Pakistan in 2015. He worked as Research Assistant in the Department of Electrical Engineering, LUMS during 2015–2016. He is currently working as Cofounder and Lead Engineer in a startup company responsible for efficient solar PV system installations in grid intermittent environments. His research interests mainly include power electronics, control systems, and renewable energy.

Laeeq Mateen received the Graduation degree in electrical engineering from Lahore University of Management Sciences (LUMS), Lahore, Pakistan in 2015. He worked as a Research Assistant in the Department of Electrical Engineering, LUMS, during 2015–2016. He is currently working as an Electrical and Automation Engineer at Nestle Pakistan Ltd., Sheikhupura, Pakistan. His research interests include the area of efficient extraction and distribution of electrical energy from renewable energy resources.

Nauman Ahmad Zaffar (M'10) currently serves as an Associate Professor and the Director of Energy and Power Systems Research Cluster at the Department of Electrical Engineering, SBASSE, Lahore University of Management Sciences, Lahore, Pakistan. He has been working with electricity distribution companies and the metering industry on power distribution management. He has also served on the Chief Minister's task force on assessment of electricity and gas theft in utility distribution companies. During his tenure at LUMS, he has been engaged in launching three power electronics startups. His research interests include smart grids and power electronic converters for integration of renewable energy resources and motor loads with an increasingly smarter grid. His primary research focus is on harnessing and efficient utilization of energy from available sources such as solar PV, solar thermal, wind and hydrokinetics to enable energy independent, integrated, and smart grid communities. He has been actively engaged in arranging and delivering national workshops in core areas of circuits, electronics, power electronics, and design of magnetics.